AIP | Applied Physics Letters

Magneto-optical harmonic susceptometry of superparamagnetic materials

Stefaan Vandendriessche, Ward Brullot, Dimitar Slavov, Ventsislav K. Valev, and Thierry Verbiest

Citation: Appl. Phys. Lett. **102**, 161903 (2013); doi: 10.1063/1.4801837
View online: http://dx.doi.org/10.1063/1.4801837
View Table of Contents: http://apl.aip.org/resource/1/APPLAB/v102/i16
Published by the American Institute of Physics.

Magneto-optical harmonic susceptometry of superparamagnetic materials

Stefaan Vandendriessche,[1] Ward Brullot,[1] Dimitar Slavov,[2] Ventsislav K. Valev,[3] and Thierry Verbiest[1]
[1]*Molecular Visualization and Photonics, KU Leuven, Celestijnenlaan 200D bus 2425, B-3001 Heverlee, Belgium*
[2]*Institute of Electronics, Bulgarian Academy of Sciences, 72 Tzarigradsko Shosse Boulevard, 1784 Sofia, Bulgaria*
[3]*Nanophotonics Centre, Cavendish Laboratory, University of Cambridge, Cambridge CB3 0HE, United Kingdom*

(Received 8 January 2013; accepted 27 March 2013; published online 23 April 2013)

We describe a technique to optically characterize superparamagnetism. Faraday rotation measurements are performed on a superparamagnetic nanocomposite using small alternating current magnetic fields. The superparamagnetism of the iron oxide nanoparticles causes signals at the uneven harmonics of the magnetic field frequency. These signals provide information on the magnetic moment of the superparamagnetic nanoparticles. Dia- and paramagnetism do not cause signals at higher harmonics, resulting in a high sensitivity to superparamagnetism, even in samples with large dia- or paramagnetic contributions. This technique provides a rapid, economical method to characterize superparamagnetism in composite samples not easily accessible by other techniques. © *2013 AIP Publishing LLC* [http://dx.doi.org/10.1063/1.4801837]

Reducing the size of magnetic particles to the nanometer range causes new effects to occur that do not exist in bulk materials.[1] An important effect is superparamagnetism, which occurs when magnetic nanoparticles are so small that they can only support a single magnetic domain.[2] Under this critical radius, the nanoparticles can be described as having a single giant magnetic spin.[3] The critical radius depends on the type of material and typically ranges from nanometers to hundreds of nanometers. For magnetite nanoparticles, it is approximately 20 nm.[4] Under this size, thermal energy is sufficient to relax the magnetization of the nanoparticles in the absence of an externally applied magnetic field on a timescale smaller than that of the experiment.[5] Shape and surface anisotropy present in the nanoparticles generally causes a uniaxial anisotropy, described by a single anisotropy energy density parameter[6] K. In the absence of an externally applied magnetic field, the particle magnetization lays along this anisotropy axis. Application of an external magnetic field initially causes the magnetization to favor one direction along the easy axis, causing a sharp increase in net magnetization of the nanoparticle sample. Higher applied magnetic fields cause the magnetization to rotate away from the anisotropy axis and towards the applied magnetic field direction.[7] This behavior can be described by the Langevin equation, and the size of the anisotropy for magnetic nanoparticles is typically such that magnetic saturation occurs at fields under 1 T.

Superparamagnetism has interesting applications in a wide variety of fields, including biomedicine,[6] bio-imaging,[8] hyperthermia,[9] magnetic fluids,[10] magnetic separation,[11] magnetic data storage,[12] and many others. Characterization of the magnetic moment μ of a superparamagnetic material is crucial for these applications. This determines amongst others the contrast of the MRI images and the effectiveness of the hyperthermia.[8] It is also important for magnetic data storage purposes,[8] and can be used for nanoparticle size determination.[13]

VSM[14] and SQUID[15] are techniques frequently used to determine hysteresis, magnetic moment, saturation magnetization, and blocking temperatures in superparamagnetic materials.[16] Alternatively, magnetization-induced second harmonic generation[17–19] is powerful for probing magnetic interfaces, and Faraday rotation can also be used to determine magnetic parameters.[20,21] However, these techniques measure the total magnetic response of the probed region of the sample, and a large dia- or paramagnetic response can make the detection of a small superparamagnetic contribution difficult and time-consuming.

Nanocomposites, composite materials where at least one constituent has a size on the order of nanometers, have become important materials with many current and future applications,[22] such as in batteries,[23] antibacterial materials,[24] biochemistry,[25] magnetic-field controlled electrical devices,[26] and many others. Nanocomposite material properties not only depend on the properties of their constituent materials but also strongly depend on their morphology, dispersion, and interfacial characteristics of the constituents.[22–27] The increase in research on nanoscale materials has been driven by the ability to characterize these materials.[28] In order to further advance the field, new characterization techniques are necessary that are accessible to many researchers.

The advantages of superparamagnetic nanoparticles in imaging have previously been demonstrated.[29] In order to improve imaging contrast, it has already been demonstrated that it is possible to perform detection at higher harmonics of the frequency of the applied magnetic field.[30,31] However, the precise relationship between the superparamagnetism of the material and the observed nonlinearities has not yet been derived.

The underlying principle of our technique (depicted in Fig. 1) relies on the nonlinear response of a superparamagnetic material to an externally applied sinusoidal magnetic field. The direction and amplitude of an externally applied magnetic field, generated by a solenoid, are modulated by an alternating current. Under the influence of this modulation, light that propagates along the direction of the magnetic field

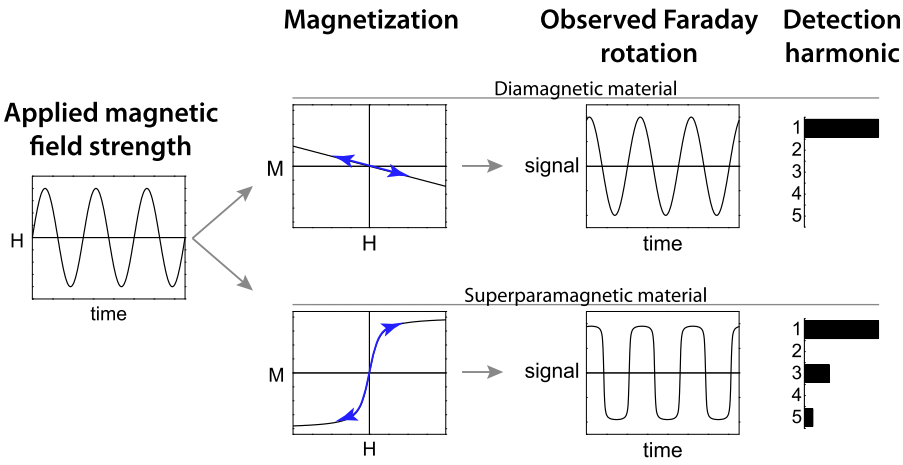

FIG. 1. The direction and amplitude of an externally applied magnetic field, generated by a solenoid, are modulated sinusoidally. At the applied magnetic field strengths, dia- and paramagnetic materials can be considered to have a linear Faraday rotation as a function of the applied magnetic field strength, while superparamagnetic materials show a Langevin equation-dependence on the applied magnetic field strength. This can be observed in the uneven higher harmonics, where the signal is solely attributable to superparamagnetism.

has its direction of polarization rotated, due to the Faraday effect. This rotation of polarization is detected by a lock-in amplifier. At the applied magnetic field strengths, maximally 18 mT, dia- and paramagnetic materials can be considered to have a linear behavior as a function of the applied magnetic field strength. As such, they only cause a signal at the fundamental frequency of the modulated magnetic field. Over the same applied magnetic field strength range, superparamagnetic materials show clear deviation from linearity due to their Langevin-dependence on the applied magnetic field strength. This deviation can be observed in the uneven higher harmonics of the modulated magnetic field, where the signal is solely attributable to superparamagnetism. This allows analysis of complex samples with very small superparamagnetic contributions. Furthermore, the size and magnetic field strength dependence of the signal at each harmonic can be correlated to the superparamagnetic properties of the material. The proposed technique for the characterization of magnetic moment in superparamagnetic materials is rapid, economical, and easily adaptable to many sample types.

Superparamagnetic iron oxide nanoparticles were synthesized using forced hydrolysis in polyol.[10] Briefly, a round-bottom flask with 37.5 ml of diethylene glycol and 25 ml of octylamine was heated to 150 °C while stirring. Separately, 2.4 g of anhydrous $FeCl_3$ was dissolved in a beaker with 3 ml of water and 10 ml of diethylene glycol. This mixture was added all at once to the round-bottom flask, which was then refluxed at 180 °C for 24 h. The resulting mixture was magnetically filtered and washed three times with acetone. After drying in a vacuum oven, a black powder of superparamagnetic nanoparticles was obtained. In order to avoid any effects of physical orientation of the superparamagnetic nanoparticles on the measurement,[32] polymer nanocomposites were synthesized with these nanoparticles. The nanoparticles were dispersed in chloroform with PMMA, typically at 10 to 15 wt %, and sonicated for 2 h. Subsequently, they were spincoated at 2000 rpm for 20 s on 1 mm thick BK7 glass slides, resulting in films of 1 to 2 μm. The resulting samples were optically isotropic. VSM measurements of a powder of the nanoparticles were performed at 300 K on an unmodified VSM Maglab setup (Oxford Instruments) (see supplementary material[37]).

In the experimental setup used to detect Faraday rotation in transmission (Fig. 2), a laser diode generates continuous wave 405 nm light, which is then linearly polarized by a GL10 Glan-Laser polarizer. This linearly polarized beam passes through a solenoid containing the sample. At the sample the beam is approximately 1 mm in diameter, at approximately 40 mW. The solenoid containing the sample is driven by a Europower EP2500 amplifier, which receives a reference sine wave at 857 Hz. The resulting sinusoidal magnetic field strength inside the solenoid causes Faraday rotation in the sample. A Wollaston prism positioned at 45° splits the light coming out of the solenoid into two beams of orthogonal polarization. Two photodiodes detect these two beams, and the resulting electronic signals are processed by a lock-in amplifier (SR830). This lock-in amplifier operates in A-B mode, subtracting the signal from the two photodiodes from each other. Measurements were performed by discretely varying the magnetic field strength and measuring the locked voltage at each harmonic for each magnetic field strength.

Faraday rotation can be described by

$$\theta = VBd, \tag{1}$$

where θ is the Faraday rotation, V is the Verdet constant, B is the magnetic field in the direction of the propagation of light, and d is the distance traveled through the magnetic field. Rewriting the magnetic field yields (in SI units)

$$\theta = V\mu_0(H + M)d \tag{2}$$

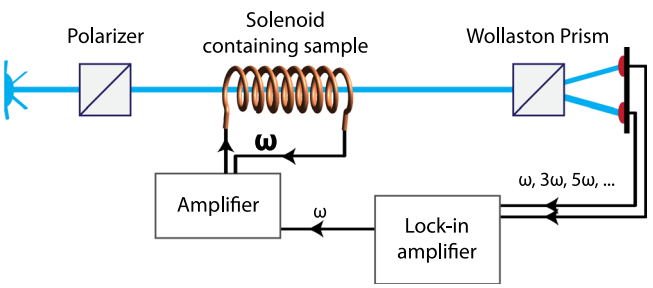

FIG. 2. In the experimental setup, a 405 nm laser diode beam is linearly polarized and then passes through a solenoid. The beam is then split into orthogonal polarizations by a Wollaston prism at 45° and is detected by photodiodes. A lock-in amplifier powers the solenoid via an amplifier at 857 Hz, producing a magnetic field in the solenoid that varies sinusoidally as a function of time.

with H the magnetic field strength, M the magnetization, and μ_0 the magnetic permeability. For dia- and paramagnetic materials the magnetization is linear as a function of the magnetic field strength, so we can write

$$\theta = V\mu_0(1+\chi)Hd \tag{3}$$

with χ the magnetic susceptibility. Using this linear relationship between Faraday rotation in a dia- or paramagnetic material and an applied magnetic field, it is possible to linearly correlate the light intensity on a photodiode to the Faraday rotation.[33]

For superparamagnetic materials, the magnetization is not a linear function of the magnetic field strength, but can be described by a Langevin function[2]

$$M = M_S L(H), \tag{4}$$

where M_S is the saturation magnetization. We can now write

$$\theta = V\mu_0(H + M_S L(H))d. \tag{5}$$

The Langevin function can be written as a function of the magnetic field strength[2]

$$L(H) = \coth(C*H) - \frac{1}{C*H}, \tag{6}$$

where $C = \mu/(k_B T)$ with kB the Boltzmann constant and mu the magnetic moment. Because $1/(C*H)$ is undefined at $H=0$, we cannot perform a Taylor expansion around this point. We can however expand $\coth(x)$ in a Laurent series around $x=0$

$$\coth(x) = \frac{1}{x} + \sum_{n=1}^{\infty} \frac{2^{2n} B_{2n} x^{2n-1}}{(2n)!}, \tag{7}$$

where B_{2n} is the $2n$th Bernoulli number. Filling this into the Langevin function, Eq. (6), yields

$$L(H) = \sum_{n=1}^{\infty} \frac{2^{2n} B_{2n} (C*H)^{2n-1}}{(2n)!}. \tag{8}$$

The applied magnetic field strength is sinusoidal in time

$$H = H_0 \sin(A), \tag{9}$$

where we write $A = \omega t + \varphi$ to lighten the notation. Filling into Eq. (8) results in

$$L(H) = \sum_{n=1}^{\infty} \frac{2^{2n} B_{2n} (CH_0)^{2n-1}}{(2n)!} \sin^{2n-1}(A). \tag{10}$$

Because $2n-1$ is odd, we can expand $\sin^{(2n-1)}(A)$ via de Moivre's formula

$$\sin^{(2n-1)}(A) = \frac{1}{2^{2n-2}} \sum_{k=0}^{n-1} (-1)^{n-1-k} \binom{2n-1}{k} \times \sin((2n-1-2k)A), \tag{11}$$

where $\binom{a}{b}$ is the binomial coefficient. Filling Eq. (11) into Eq. (10) yields

$$L(H) = \sum_{n=1}^{\infty} \left[\frac{4 * B_{2n} (CH_0)^{2n-1}}{(2n)!} \sum_{k=0}^{n-1} (-1)^{n-1-k} \binom{2n-1}{k} \times \sin((2n-1-2k)A) \right] \tag{12}$$

and finally we fill Eq. (12) into Eq. (5)

$$\theta = V\mu_0 \left(H_0 \sin(A) + M_S \sum_{n=1}^{\infty} \left[\frac{4 * B_{2n} (CH_0)^{2n-1}}{(2n)!} \times \sum_{k=0}^{n-1} (-1)^{n-1-k} \binom{2n-1}{k} \sin((2n-1-2k)A) \right] \right) d. \tag{13}$$

We see that, in contrast to Eq. (3) for dia- and paramagnetic materials, the observed Faraday rotation θ contains components at higher harmonics of the frequency of the magnetic field. Because $2n-1-2k$ is uneven, we see that there will only be uneven harmonics present. Using Eq. (13), we can now determine what signal will be present at each harmonic for a given superparamagnetic sample. Explicit derivations for the first and the third harmonic can be found in the supplementary material. Neglecting nonlinearities at very low fields reduces Eq. (13) to a linear relation between the signal at the fundamental frequency of the applied magnetic field and the amplitude of the applied magnetic field, allowing determination of the Verdet constant of the material.[10,21,34]

For the measured superparamagnetic nanocomposite, a clear signal was detected on the lock-in amplifier for all uneven harmonics until the 13th harmonic, while no signal was observed for any even harmonic. Purely dia- and paramagnetic samples only produced a measurable signal at the fundamental frequency. The signal for the superparamagnetic nanocomposite divided by the dc voltage on the photodiodes is plotted as a function of the magnetic field in Fig. 3 for the first to the seventh harmonic.

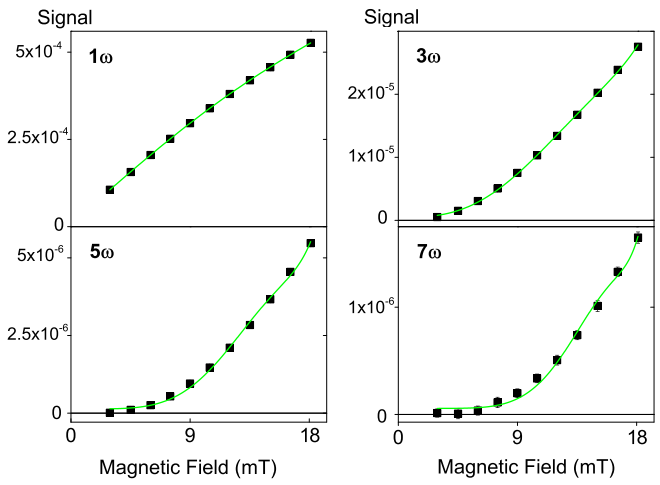

FIG. 3. A clear non-linear dependence is seen in the signal of the superparamagnetic nanocomposite as a function of the magnetic field, with higher order harmonics displaying higher order nonlinearities in the magnetic field. Fitting is performed to equations derived from Eq. (13), allowing for four magnetic field strength dependent terms per fit.

TABLE I. Value of C for fits to Eq. (13) for each measured harmonic of the superparamagnetic nanocomposite.

Measured harmonic	C (T^{-1}) from fitting to Eq. (13)	±
3	163.16057	13.29059
5	153.29697	13.51621
7	143.12684	12.48853
9	132.8965	11.4159
11	127.12693	10.72927
13	119.17883	9.68399

Fitting the observed signal as a function of the applied magnetic field strength to Eq. (13) yields a value for C, the constant in the Langevin equation (6). When performing these fittings, care needs to be taken to avoid overfitting.[35] Using too many terms in the fit attributes too much importance to noise in the data, resulting in incorrect fits (supplementary material Fig. 2) For our data, it was empirically determined that the optimal number of terms was four. The resulting fits are displayed in Fig. 3, and the associated values for C are displayed in Table I.

These C values can be related to the magnetic properties of the material via[2] $C = \mu/(k_B T)$; this can be interpreted as a ratio of the magnetic moment to the thermal energy. We can now compare the measured C to that derived from VSM measurements performed on a powder of the nanoparticles from $-20\,\mathrm{mT}$ to $20\,\mathrm{mT}$, where $C = 177\mathrm{T}^{-1}$. This corresponds quite well to the values obtained from our characterization technique. However, this is larger than the values typically reported in literature for these nanoparticles, which, for this size of iron oxide nanoparticles, range[13] from $25\mathrm{T}^{-1}$ to $45\mathrm{T}^{-1}$. The reason for this discrepancy lies in the small range of the magnetic field strength measured. When the VSM hysteresis is acquired from $3\,\mathrm{T}$ to $-3\,\mathrm{T}$, we obtain $C = 40\mathrm{T}^{-1}$. As the range of magnetic field strength is decreased, the fit value for C increases. This dependence of C on the magnetic field strength range is due to the fact that the particles deviate from ideal Langevin behavior.

Our technique is more applicable to small magnetic field strengths than VSM measurements, which tend to be optimized for measurements at large magnetic field strengths. See supplementary material for an example of a VSM curve at a small magnetic field. Our technique on the other hand excels at smaller magnetic field strengths.

An important application of our technique is the observation of non-ideal superparamagnetic behavior. For ideal Langevin behavior, the C values for each harmonic in Table I would be equal. From this single C value, the magnetic moment of the nanoparticles can be calculated. However, the value of C differs for each harmonic. The deviations from the ideal values of C can be used to acquire information on the non-idealities present in the sample. Possible causes of non-idealities are the size distribution of the nanoparticles, inter-particle interactions, or surface effects.[36] Our technique is well-suited to further analyze these non-idealities.

Superparamagnetism is an important effect in magnetic nanoparticles. While magnetism in materials can be characterized by a variety of techniques, characterizing superparamagnetism in thin film samples with a large dia- or paramagnetic contribution remains difficult. We have demonstrated an optical magnetization characterization uniquely sensitive to superparamagnetism.

For the investigated superparamagnetic iron oxide polymer nanocomposite, a clear signal was observed for all uneven harmonics until the 13th harmonic, while no signal was observed for any even harmonic. Solely dia- and paramagnetic samples only produced a measurable signal at the fundamental frequency, with no signal at any higher harmonic. Our characterization technique is rapid and economical, and the resulting values provide information on the superparamagnetism present in the sample.

S.V. is grateful for financial support from FWO-Vlaanderen. We are grateful to the University of Leuven (GOA and Research fund) for financial support. W.B. received funding from the Agency for Innovation by Science and Technology (IWT) Flanders. V.K.V. acknowledges financial support from the EPSRC Grant EP/G060649/1 and the VS.040.10N grant from the BAS and the FWO. We acknowledge useful discussions with M. Bloemen, P.-J. Demeyer, and M. Vanbel.

[1]S. Bedanta and W. Kleemann, J. Phys. D: Appl. Phys. **42**, 013001 (2009).
[2]M. Knobel, W. C. Nunes, L. M. Socolovsky, E. De Biasi, J. M. Vargas, and J. C. Denardin, J. Nanosci. Nanotechnol. **8**, 2836 (2008).
[3]R. H. Kodama, J. Magn. Magn. Mater. **200**, 359 (1999).
[4]L. Zhou, J. Yuan, and Y. Wei, J. Mater. Chem. **21**, 2823 (2011).
[5]D. X. Chen, O. Pascu, A. Roig, and A. Sanchez, J. Magn. Magn. Mater. **322**, 3834 (2010).
[6]Q. A. Pankhurst, J. Connolly, S. K. Jones, and J. Dobson, J. Phys. D: Appl. Phys. **36**, R167 (2003).
[7]X. Batlle and A. Labarta, J. Phys. D: Appl. Phys. **35**, R15 (2002).
[8]N. A. Frey, S. Peng, K. Cheng, and S. Sun, Chem. Soc. Rev. **38**, 2532 (2009).
[9]A. K. Gupta and M. Gupta, Biomaterials **26**, 3995 (2005).
[10]W. Brullot, N. K. Reddy, J. Wouters, V. K. Valev, B. Goderis, J. Vermant, and T. Verbiest, J. Magn. Magn. Mater. **324**, 1919 (2012).
[11]U. Jeong, X. Teng, Y. Wang, H. Yang, and Y. Xia, Adv. Mater. **19**, 33 (2007).
[12]A. Moser, K. Takano, D. T. Margulies, M. Albrecht, Y. Sonobe, Y. Ikeda, S. Sun, and E. E. Fullerton, J. Phys. D: Appl. Phys. **35**, R157 (2002).
[13]D. X. Chen, A. Sanchez, E. Taboada, A. Roig, N. Sun, and H. C. Gu, J. Appl. Phys. **105**, 083924 (2009).
[14]S. Foner, Rev. Sci. Instrum. **30**, 548 (1959).
[15]S. Vandeleene, M. Jivanescu, A. Stesmans, J. Cuppens, M. J. Van Bael, H. Yamada, N. Sato, T. Verbiest, and G. Koeckelberghs, Macromolecules **43**, 2910 (2010).
[16]V. Salgueiriño-Maceira, M. A. Correa-Duarte, E. Duman, and M. Farle, J. Magn. Magn. Mater. **299**, 467 (2006).
[17]S. Vandendriessche, V. K. Valev, and T. Verbiest, Appl. Opt. **51**, 209 (2012).
[18]V. K. Valev, A. Kirilyuk, F. Dalla Longa, J. T. Kohlhepp, B. Koopmans, and T. Rasing, Phys. Rev. B **75**, 012401 (2007).
[19]H. A. Wierenga, M. W. J. Prins, D. L. Abraham, and T. Rasing, Phys. Rev. B **50**, 1282 (1994).
[20]G. Rosa, H. Guerrero, D. Levy, A. Alvarez-Herrero, and R. P. del Real, J. Appl. Phys. **97**, 064314 (2005).
[21]S. Vandendriessche, V. K. Valev, and T. Verbiest, Phys. Chem. Chem. Phys. **14**, 1860 (2012).
[22]F. Hussain, M. Hojjati, M. Okamoto, and R. E. Gorga, J. Compos. Mater. **40**, 1511 (2006).
[23]J. B. Goodenough and Y. Kim, Chem. Mater. **22**, 587 (2010).
[24]Y. F. Joya, Z. Liu, K. S. Joya, and T. Wang, Nanotechnology **23**, 495708 (2012).
[25]J. W. Thompson, H. A. Stretz, P. E. Arce, H. Gao, H. J. Ploehn, and J. He, J. Appl. Polym. Sci. **126**, 1600 (2012).
[26]H. Wu, B. Xu, A. Liu, and G. Chai, J. Phys. D: Appl. Phys. **45**, 455306 (2012).

[27]G. Vleminckx, S. Bose, J. Leys, J. Vermant, M. Wübbenhorst, A. A. Abdala, C. Macosko, and P. Moldenaers, ACS Appl. Mater. Interfaces **3**, 3172 (2011).
[28]"Nanoscience and nanotechnologies," The Royal Society & The Royal Academy of Engineering Technical Report, 2004.
[29]*Magnetic Particle Imaging: A Novel SPIO Nanoparticle Imaging Technique*, edited by T. M. Buzug and J. Borgert (Springer, Berlin, 2012), Vol. 140.
[30]B. Gleich and J. Weizenecker, Nature **435**, 1214 (2005).
[31]S.-H. Chung, M. Grimsditch, A. Hoffmann, S. D. Bader, J. Xie, S. Peng, and S. Sun, J. Magn. Magn. Mater. **320**, 91 (2008).
[32]M. Xu and P. J. Ridler, J. Appl. Phys. **82**, 326 (1997).
[33]V. K. Valev, J. Wouters, and T. Verbiest, Eur. J. Phys. **29**, 1099 (2008).
[34]A. Jain, J. Kumar, F. Zhou, and L. Li, Am. J. Phys. **67**(8), 714 (1999).
[35]D. M. Hawkins, J. Chem. Inf. Comput. Sci. **44**, 1 (2004).
[36]G. F. Goya, T. S. Berquo, F. C. Fonseca, and M. P. Morales, J. Appl. Phys. **94**, 3520 (2003).
[37]See supplementary material at http://dx.doi.org/10.1063/1.4801837 for an example of a VSM curve at a small magnetic field.